

PAPER • OPEN ACCESS

Surface oxidation of $\text{Ti}_3\text{C}_2\text{T}_x$ enhances the catalytic activity of supported platinum nanoparticles in ammonia borane hydrolysis

To cite this article: Thierry K Slot *et al* 2020 *2D Mater.* **8** 015001

View the [article online](#) for updates and enhancements.

2D Materials



PAPER

OPEN ACCESS

RECEIVED
28 May 2020

REVISED
23 July 2020

ACCEPTED FOR PUBLICATION
3 August 2020




PUBLISHED
6 October 2020

Original content from this work may be used under the terms of the [Creative Commons Attribution 4.0 licence](https://creativecommons.org/licenses/by/4.0/).

Any further distribution of this work must maintain attribution to the author(s) and the title of the work, journal citation and DOI.



Surface oxidation of $Ti_3C_2T_x$ enhances the catalytic activity of supported platinum nanoparticles in ammonia borane hydrolysis

Thierry K Slot¹ , Fang Yue², Hualong Xu², Enrique V Ramos-Fernandez³, Antonio Sepúlveda-Escribano³, Zdeněk Sofer⁴, Gadi Rothenberg¹  and N Raveendran Shiju¹ 

¹ Van 't Hoff Institute for Molecular Sciences, University of Amsterdam, Science Park 904, Amsterdam, The Netherlands

² Department of Chemistry, Shanghai Key Laboratory of Molecular Catalysis and Innovative Materials and Laboratory of Advanced Materials, Fudan University, Shanghai, People's Republic of China

³ Laboratorio de Materiales Avanzados. Departamento de Química Inorgánica - Instituto Universitario de Materiales de Alicante, Universidad de Alicante, Alicante, Spain

⁴ Department of Inorganic Chemistry, University of Chemistry and Technology, Prague Technicka 5, 16628 Prague 6, Czech Republic

E-mail: n.r.shiju@uva.nl

Keywords: heterogeneous catalysis, 2D materials, MAX phase, metal-support interactions, rutile titania, ozone

Abstract

MXenes, first discovered in 2011, are two-dimensional transition metal carbides or nitrides. Because of their interesting electrical and optical properties, they are studied for applications in batteries, supercapacitors and electrocatalysis. However, MXenes are rarely used in heterogeneous catalysis and, to our knowledge, there are no reports on the use of oxidized MXenes in catalysis. Here we used $Ti_3C_2T_x$ -derived materials as supports for platinum nanoparticles and studied their effectiveness for the hydrolysis of ammonia borane, which is a promising hydrogen carrier. Hydrogen can be released from ammonia borane through catalytic hydrolysis. Most heterogeneous catalysts reported for this purpose contain a noble metal supported on a metal oxide support. The interaction between the metal and the support is important in determining the catalytic performance. Our results show that the electronic environment of platinum can be modified by oxidising the surface of MXene, thus providing a new way of developing active catalysts. Oxidising agents such as water and ozone can be used for this purpose. This electronic modification enhances the catalytic activity of platinum for ammonia borane hydrolysis, which is relevant for other reactions related to energy production/storage.

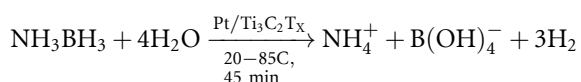
1. Introduction

MXenes are novel two-dimensional transition metal carbides, nitrides or carbonitrides [1]. Their structure is defined as $M_{n+1}X_nT_x$, where M is an early transition metal, X is carbon and/or nitrogen, and T stands for a terminating functional group [2]. They are produced by extracting the 'A' layers from MAX phases, which are layered ternary transition metal carbides [2–5]. MXenes have been studied extensively in the past few years, especially for electrocatalysis [6–13]. Their thermocatalytic applications, however, are less known. Li *et al* recently showed that MXenes are promising supports for nanoparticle-based catalysts and they can change the nature of the active sites, making them highly selective towards C–H

activation [14, 15]. Here, we use a different approach: we reasoned that oxidizing the surface of MXenes can influence the metal supported on it, thereby modulating the catalytic activity when compared to the metal supported on pristine MXene. Taking ammonia borane hydrolysis as a probe reaction, we show that this oxidation approach enhances the catalytic activity of supported metal particles. Usually, the oxidation leads to particles of anatase (TiO_2) along the edges of the flakes and the basal planes [16–18]. Reaction conditions such as temperature and solvent choice can control the structure of the resulting titania ranging from simple layers to complex nanostructures [17, 19]. Here we used, for the first time, controlled oxidation with ozone, which resulted mainly in rutile titania on a partially exfoliated $Ti_3C_2T_x$ MXene

surface. Impregnating this surface with a platinum salt gave stable subnanometre platinum particles that were highly active as ammonia borane hydrolysis catalysts.

Ammonia borane hydrolysis is an emerging method for on-demand hydrogen generation. While hydrogen is acknowledged as the fuel of the future [20–23], its current storage and transportation methods have serious drawbacks. Hydrogen storage should be safe, easy, reversible, and should have a high gravimetric/volumetric capacity. This makes chemical hydrogen storage a promising option [24–26]. Recently, ammonia borane (NH_3BH_3) attracted considerable attention because of its high hydrogen density, stability and relative ease of hydrolysis [27–33]. Here, we show how modifications on the MXene surface can influence the reactivity of Pt particles towards H_2 generation from ammonia borane. (equation 1)



2. Experimental

2.1. MXene ($\text{Ti}_3\text{C}_2\text{T}_x$) synthesis

All chemicals were obtained from commercial sources and were used as received. Ti_3AlC_2 was obtained from Carbon-Ukraine and had a purity >95% (verified by X-ray diffraction, XRD). Ti_3AlC_2 was etched with HF (40 wt%) for 7 d under continuous stirring at room temperature. The mixture was repeatedly centrifuged and washed with deionized water until the pH of the supernatant was neutral. The powder obtained after this procedure was dried under vacuum. The resulting material is denoted as $\text{Ti}_3\text{C}_2\text{T}_x$.

2.2. Synthesis of MXene composites

2.2.1 Ozone treatment (MXene- O_3)

$\text{Ti}_3\text{C}_2\text{T}_x$ (100 mg) was suspended into chloroform (10 ml) and stirred at 1000 rpm. Ozone was bubbled through the suspension at a rate of 25 ml min^{-1} for 1 h at 22°C . The resulting mixture was centrifuged ($3000 \times g$) and washed twice with chloroform. The product was dried under vacuum at 30°C for 16 h.

2.2.2 Hydrothermal treatment of MXene (MXene- H_2O)

$\text{Ti}_3\text{C}_2\text{T}_x$ (100 mg) and water (25 ml) were added to a 75 ml autoclave. The mixture was stirred (600 rpm) and heated to 285°C within 20 min and held at this temperature for 30 min. The autoclave was cooled to 25°C . The resulting MXene- TiO_2 composite was washed five times with water and once with ethanol, and then dried under vacuum at 30°C for 16 h.

2.2.3 Hydrogen peroxide treatment of MXene (MXene- H_2O_2)

$\text{Ti}_3\text{C}_2\text{T}_x$ (50 mg) and ethanol (25 ml) were added to a 100 ml round-bottom flask. The mixture was stirred and heated to 70°C , when 30% H_2O_2 (1.0 ml) was slowly added. The mixture was stirred at 70°C for 2.5 h. The remaining solid material was washed five times with water and once with ethanol, and then dried under vacuum at 30°C for 16 h.

2.3. Platinum impregnation procedure

The impregnation procedure has been adapted from the double-solvent method [34]. Support material (100 mg) was loaded into a 2 ml vial with 1 ml of *n*-hexane. Tetra-amine platinum nitrate (50.1 mg) was dissolved in water (1.00 ml) and 40 l of this solution was added to the suspension under stirring (2000 rpm). The mixture was stirred for 16 h, after which the solvent was decanted and the residue was dried in air for 3 h. The impregnated material was further dried at 80°C for 3 h, 120°C for 2 h, and then heat-treated in nitrogen at 250°C for 1 h. Finally, the samples were reduced at 250°C for 1 h in a 250 ml min^{-1} stream of 10% ($v v^{-1}$) hydrogen in nitrogen.

2.4. Catalytic testing

A 10 ml glass reactor was filled with catalyst (2.0 mg) and water (8 ml). The reactor was mounted in the bubble counter setup [35]. The reactor was then cooled to 20°C on an ice bath after purging with H_2 for 5 min. Ammonia borane (2 M, 400 l) was injected into the reactor through a glass capillary directly into the solution. The sample was stirred continuously at 600 rpm with a $8 \times 3 \text{ mm}$ stirring bar. The sample was heated at a ramp rate of 2°C min^{-1} to 85°C , and held there until no more gas was evolving from the reaction. Hydrogen production was monitored throughout the experiment by counting bubbles forming in a hexadecane medium. A blank experiment with only water (8.4 ml) was also performed to record the gas volume increase due to gas expansion and increasing vapour pressure of the solvent. This blank was subtracted from all experiments.

2.5. Characterization

N_2 adsorption isotherms were recorded on a Thermo Scientific Surfer instrument at -196°C . All samples were completely degassed under a high vacuum ($<10^{-4}$ torr) at 200°C for 6 h prior to each measurement.

Confocal Raman spectra were recorded at 532 nm using a Renishaw (Wotton-under-Edge, United Kingdom) InVia Reflex Raman microscope with a 532 nm frequency-doubled Nd:YAG excitation source in combination with a $1800 \text{ lines mm}^{-1}$ grating, and

Table 1. Overview of physical and catalytic parameters for the MXene composite catalysts.

Material	TOF ^[a] 30 °C (min ⁻¹)	E _a ^[b] (kJ mol ⁻¹)	Pt particle size ^[c] (nm)	SSA ^[d] (m ² g ⁻¹)
Pt/MXene	39	60	1.6	24
Pt/MXene-O ₃	265	69	0.6	30
Pt/MXene-H ₂ O	272	99	1.5	10
Pt/TiO ₂ -anatase	38	64	—	5

^[a] Calculated from H₂ production using reaction order of 0.15 in ammonia borane.

^[b] Apparent activation energy obtained from triplicate run data up to 20% conversion of ammonia borane.

^[c] Calculated from HAADF-TEM data statistical analysis observing >100 particles.

^[d] SSA = Specific Surface Area

a Peltier-cooled CCD detector (203 K). The instrument included a Leica light microscope with a 50x air objective. The 521 cm⁻¹ Raman shift of asilicon standard was used to verify the spectral calibration of the system. X-ray photoelectron spectroscopy (XPS) analysis was carried out in a K-Alpha Spectrometer (Thermo-Scientific). The assignment of the C 1s binding energies was done according to the criteria used by Ganguly *et al.*: 284.5 eV for C=C (aromatic double bonds), 285.5 eV for C–OH and sp³ C–C, 286.5 eV for epoxy, 287.5 for sp² C=O (carbonyls, lactones), and 289 eV for carboxylic groups [36]. X-ray diffraction (XRD) measurements were carried out on a Rigaku Miniflex X-ray diffractometer from 4° to 70° using a 2.0° min⁻¹ angular velocity.

Scanning electron microscope (SEM) images were taken by a FEI Verios 460 using a 5 kV accelerating voltage. High resolution transmission electron microscopy (HRTEM) images were recorded on a FEI Tecnai G2 F20 S-Twin high-resolution transmission electron microscope working at 200 kV (point resolution: 0.24 nm, lattice resolution 0.102 nm, information resolution 0.14 nm). STEM-EDS images were recorded using an EDS detector with energy resolution <127 eV and a resolution of 0.20 nm.

3. Results and discussion

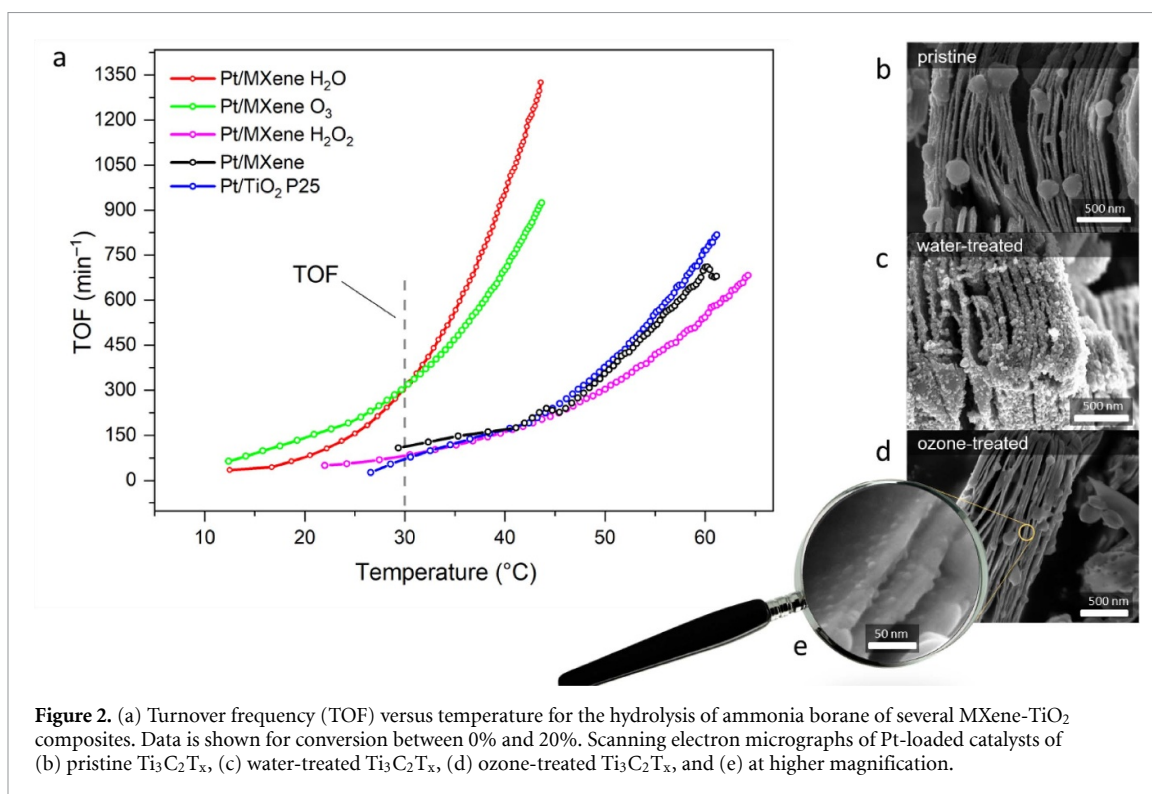
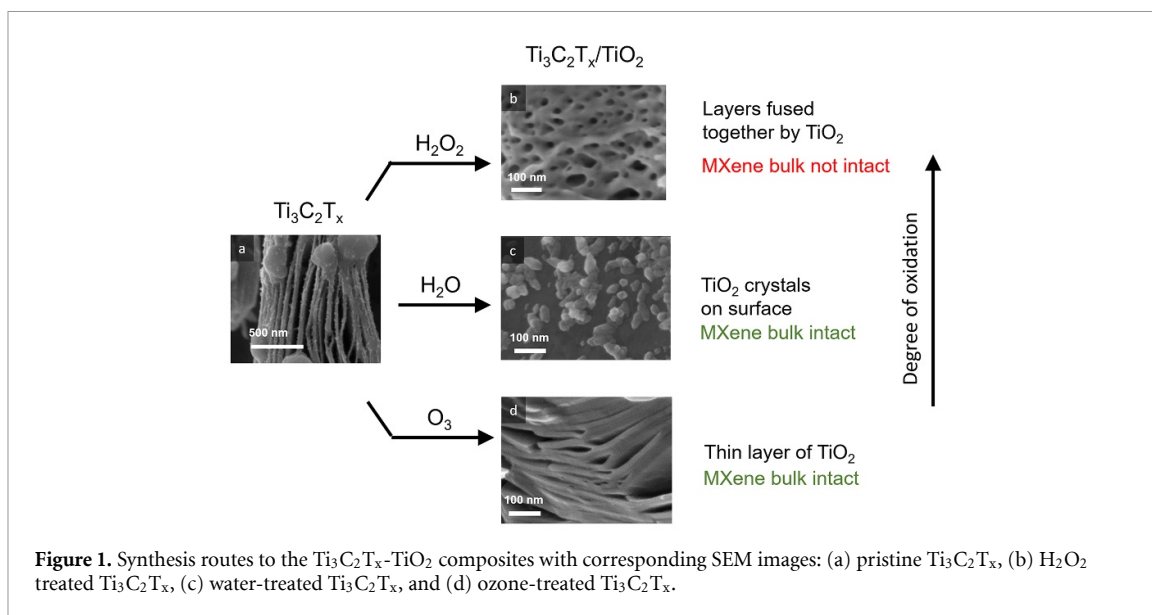
First, we studied the ozone oxidation of Ti₃C₂T_x MXene. We suspended Ti₃C₂T_x in chloroform and then bubbled ozone at controlled conditions (see experimental section for details). For comparison, we also used two other oxidative treatments: hydrothermal treatment at 200 °C, and treatment with H₂O₂ (see figure 1). These oxidative treatments changed the surface of MXene significantly (*cf.* SEM images in figure 1). We then impregnated all three samples with platinum using the double-solvent method (water in hexanes) [34]. The samples were dried at 80 °C, heat-treated at 250 °C in nitrogen and finally reduced at 250 °C using 10% hydrogen in nitrogen. The final Pt loading was 1 wt%.

We then tested these catalysts in ammonia borane hydrolysis [37–46]. The progress of this reaction can be easily monitored by measuring the volume of H₂ produced, using our new gas quantification

setup [35]. This device allows to precisely record gas production with time, recording thousands of data points from a single reaction. Additionally, ammonia borane hydrolysis has a very low concentration dependence on ammonia borane (partial reaction order $n = 0.1$ – 0.2), allowing us to gather turnover frequency (TOF) data with respect to temperature as well. All TOFs were calculated assuming the total weight of Pt is available for catalysis (in practice, the TOF values per available Pt atom would be somewhat higher, considering the small size of the clusters).

Control reactions showed that the catalytic activity of pristine or oxidized MXenes without platinum was negligible. Platinum supported on untreated MXene (Pt/MXene) gave a TOF of 40 min⁻¹. Supporting Pt on ozone-treated MXene (Pt/MXene-O₃) increased the TOF seven-fold to 250–300 min⁻¹ (see figure 2a). This shows that the surface treatment influences the reactivity significantly. Pt supported on water-treated MXene (Pt/MXene-H₂O) also gave a high TOF (figure 2a). The apparent activation energy (E_a) calculated from Arrhenius plots is 69 kJ mol⁻¹ for Pt/MXene-O₃. The peroxide-treated MXene did not show any improvement compared to the milder oxidation methods. The apparent activation energy of Pt/MXene-H₂O is higher (99 kJ mol⁻¹), suggesting a different rate-determining step (in the case of a single reaction step) or a change of the environment around the active site.

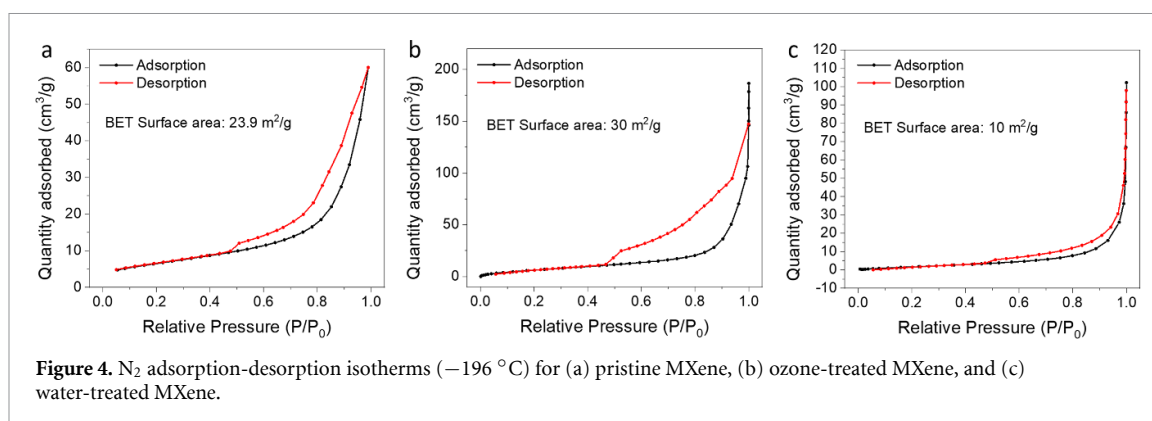
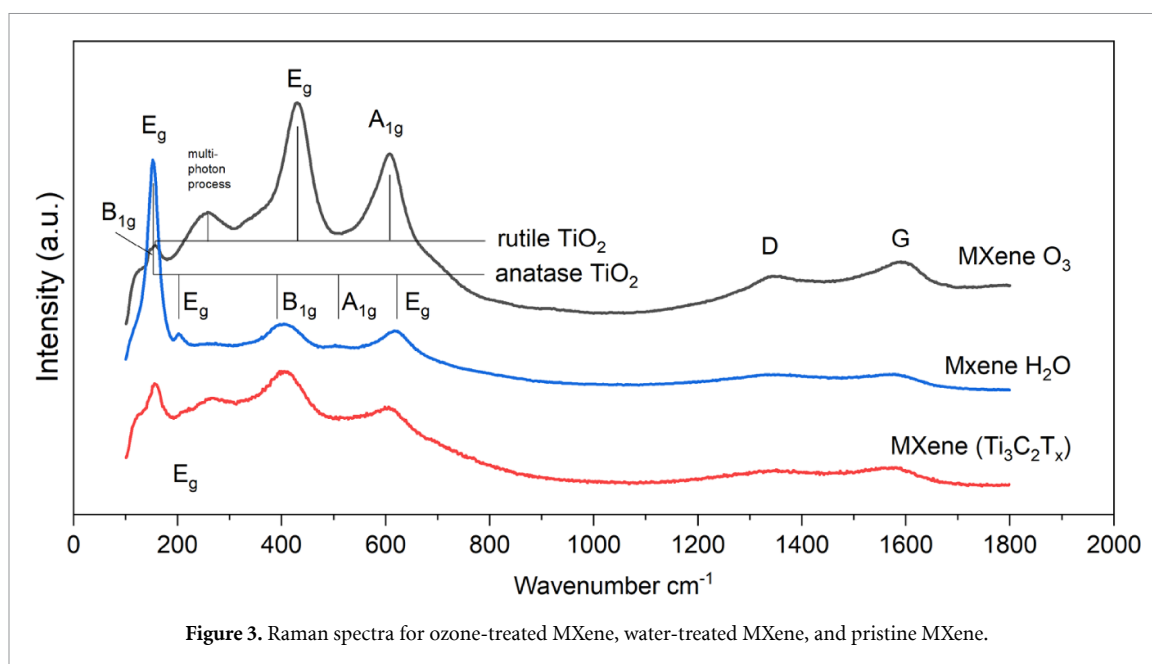
We then studied the structure of the modified catalysts using several characterization techniques. An overview of the catalyst properties is shown in table 1. Interestingly, SEM study showed no major changes after ozone exposure of Ti₃C₂T_x MXene (*cf.* figures 2d and b). In contrast, we saw major changes on the surface of MXene when treated hydrothermally or with H₂O₂ (figure 1b), proving that the surface structure changes depend on the treatment method. Oxidation of Ti₃C₂T_x MXene with water gave crystalline structures on the surface [18, 19, 47]. These structures mainly consist of anatase titania. Peroxide treatment completely converted the MXene bulk into amorphous titania and, consequently, did not show any improved reactivity. This suggests that a MXene lattice core is required



for reactivity enhancement. XPS studies showed that the surface is oxidised to titanium oxide in all oxidation treatments (figures 7b and c). Each oxidation method gives different titania phase compositions (figure 5). Ozone treatment results in rutile and amorphous phases. Hydrothermal treatment gives both rutile and anatase, while hydrogen peroxide gives an amorphous material, comparable to bulk TiO_2 . The exact reason for these differences is unclear. We think this is related to the oxidant strength and/or solvent type. Transmission electron micrographs (TEM) revealed an oxidised surface layer of around 10–15 nm thickness for the ozone treated samples

(figure 6d). XRD revealed that ozone treatment generated a crystalline phase corresponding to rutile titania (figure 5). This is interesting, as rutile TiO_2 usually forms at higher temperatures while our ozone experiments were run at ambient temperature. Other oxidation treatments predominantly led to the formation of anatase titania [16, 19]. As far as we know, this is the first report showing that oxidation with ozone forms rutile titania on MXene surfaces.

Raman spectroscopy showed the characteristic TiO_2 bands as well as the D/G band corresponding to graphitic layers (see figure 3). For the ozone-treated

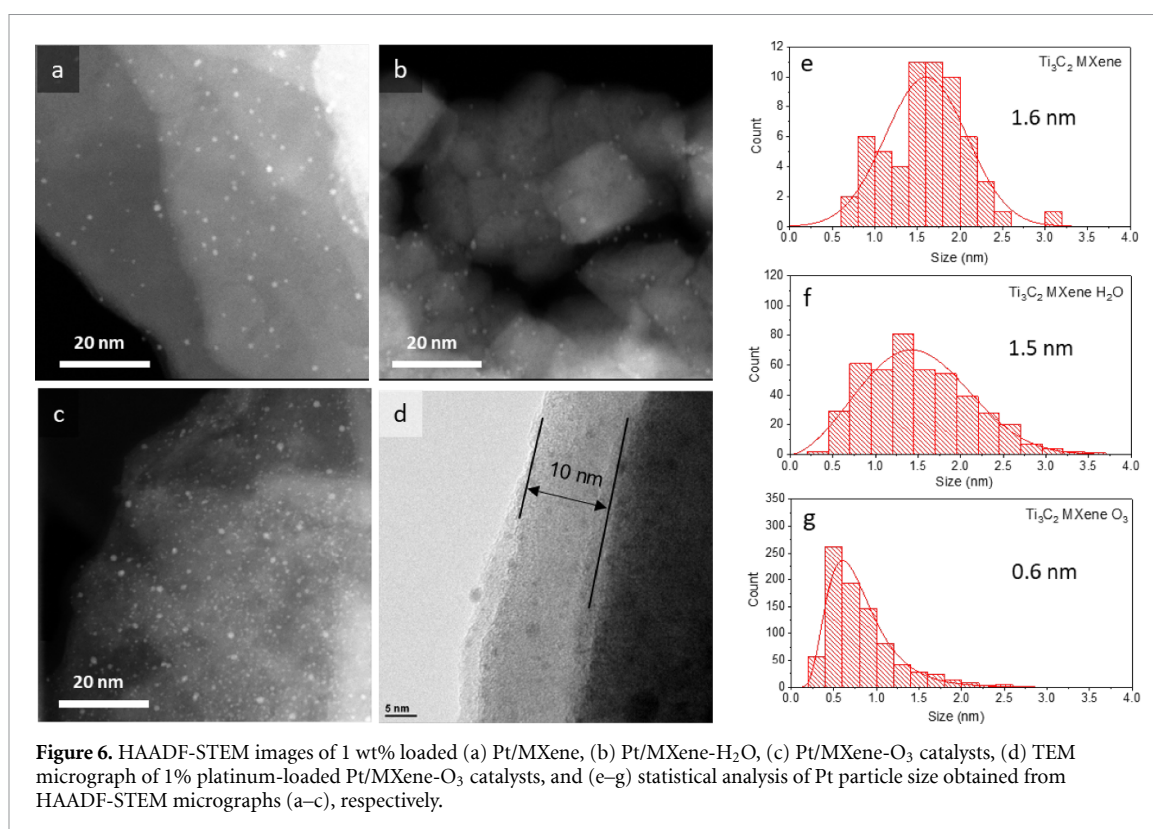
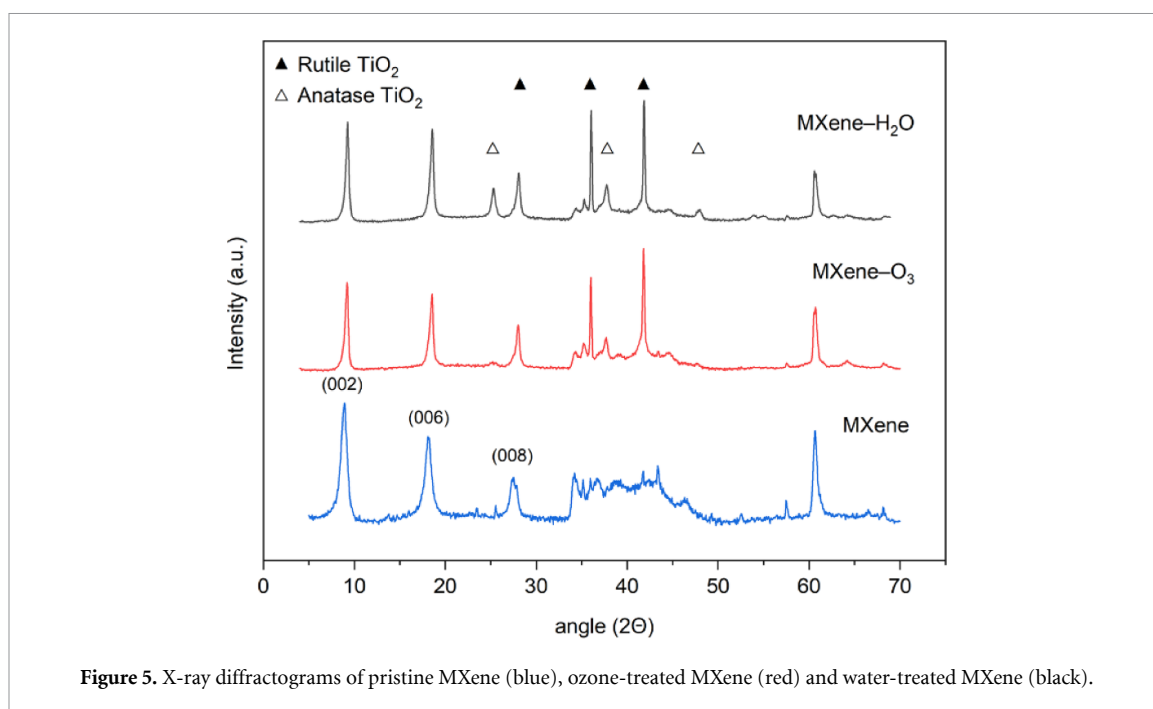


sample, we observed strong rutile TiO₂ signals at 430 cm^{−1} (E_g) and 607 cm^{−1} (A_{1g}), confirming the presence of rutile titania at the surface [48–50]. The water-treated sample showed strong anatase TiO₂ signals at 152 and 204 cm^{−1} (E_g) while the remaining signals at 408, 506 and 621 cm^{−1} overlap with those of MXene.

The N₂ adsorption measurements for pristine and ozone-treated MXene gave BET surface areas of 24 and 30 m² g^{−1}, respectively (figure 4). A MXene-TiO₂ composite was reported to have a surface area of 32 m² g^{−1} in previous work [51]. Literature estimates range from 8 to 30 m² g^{−1} for multilayer Ti₃C₂T_x, depending on the degree of delamination [51–53].

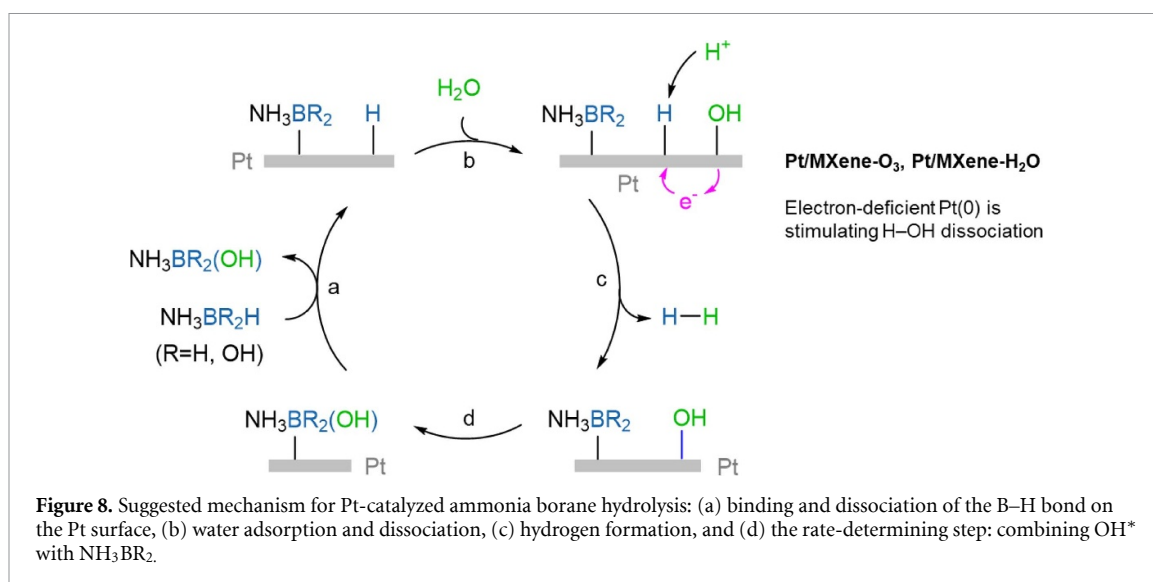
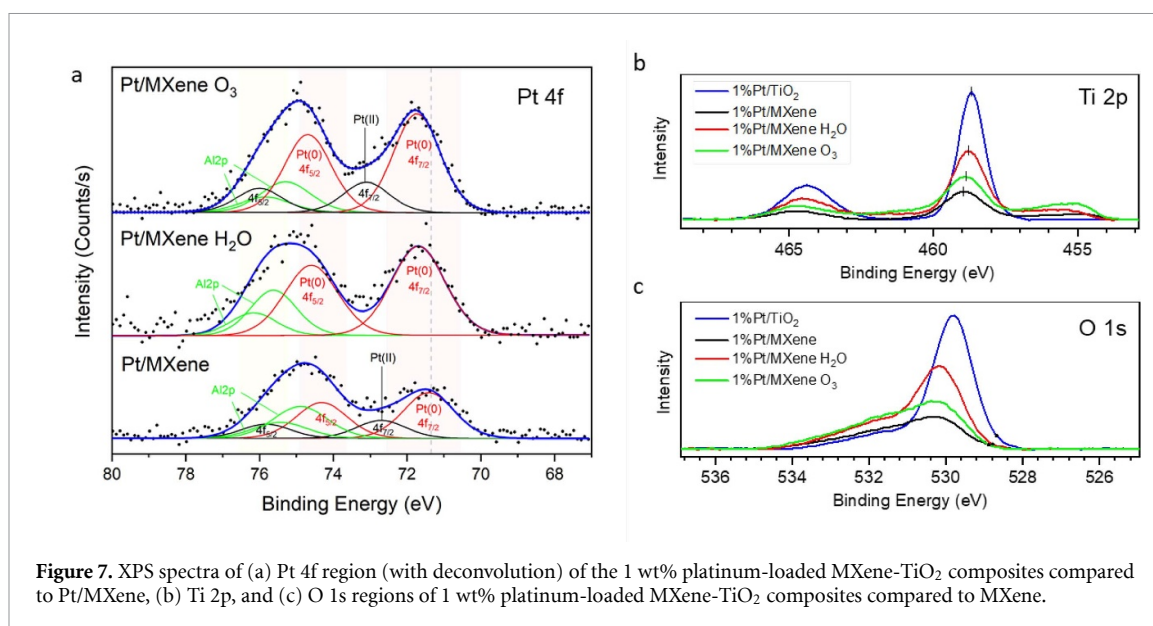
Electron microscopy studies of Pt/MXene-O₃ and Pt/MXene-H₂O showed a uniform distribution of Pt particles (see figure 6). For Pt/MXene-O₃, the Pt particles are also well dispersed within the space between the MXene layers as shown by SEM (figure 2e). However, particle size distribution studies showed a major difference (figures 6e and f). A relatively uniform size distribution with an

average particle size around 1.5–1.6 nm was observed for Pt/MXene and Pt/MXene-H₂O. However, the Pt particles on Pt/MXene-O₃ were smaller, with an average size of 0.6 nm. Thus, the characterization data show that our unique ozone treatment method gives a surface enriched with rutile titania and the Pt nanoparticles deposited on this surface remain small in size. In previous work, we observed the retention of small particle size when Ru was deposited on bulk rutile titania. However, in that case a lattice matching was possible between the rutile RuO₂ intermediate and rutile TiO₂ [54]. Such matching is not expected here, so the small particle size cannot be explained by it. Ozone is very reactive, and there is no water to facilitate crystallisation, as in the case of the MXene-H₂O material. We expect this mechanism to form a rough amorphous/rutile surface, with many defect sites, possibly even oxygen vacancies. The rough surface likely hinders the aggregation of Pt atoms during particle formation, allowing the structure to retain a small Pt particle size. Chen *et al* studied the relation between catalytic activity of Pt and its particle size on carbon nanotubes,



suggesting an optimal Pt particle size of 1.8 nm [55]. For smaller particles, they observed a decreasing TOF. However, their support does not interact with the Pt particles. We *do* observe very good activity at small sizes, especially for the ozone-treated catalyst. This suggests that the high TOF is the result of an electronic interaction between the Pt particles and the oxidised MXene support. The ozone-treated and water-treated catalysts are equally active, even though their particle sizes differ. This shows that

particle-size effects are less important here. TEM data shows that platinum particles are deposited on the surface titania layer, apparently with no direct contact with the bulk MXene (figure 6d). To compare the activity of this material with bulk titania, we prepared and tested a Pt/TiO₂ catalyst, using a commercial bulk titania (Degussa P25, anatase:rutile ~3:1) as the support. However, this catalyst was less active than the oxidized MXene catalysts (figure 2a). This suggests that the electronic nature of Pt is



modified on oxidized Ti₃C₂T_x MXene, enhancing its catalytic activity. Though the Pt nanoparticles are supported on the titania layer, the underlying bulk MXene has an influence, making it different from Pt/bulk titania catalysts.

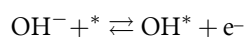
To gain further insight, we studied the electronic structure of the Pt/MXene catalysts with XPS. The results confirmed that the surfaces of all of the oxidised MXene samples contain TiO₂. The Pt 4f XPS spectra and their deconvolutions show that the binding energy shifts upward by 0.4 eV (figure 7a) for Pt/MXene-O₃ and Pt/MXene-H₂O. This indicates that Pt is in a higher oxidation state when it is deposited on oxidised MXene. This shift is even more pronounced than what was previously reported for Pt/Ti₃C₂T_x [14]. This shift also correlates with the high catalytic activity of Pt/MXene-O₃ and Pt/MXene-H₂O (figure 2a). If the electron transfer is from the TiO₂ layer to the supported particle, a

shift towards lower binding energy is expected. We may assume that the reverse occurs in this case, making the Pt nanoparticles more electron deficient. XPS analysis shows that the titania surface is electron-deficient compared to bulk titania (figures 7b and c). We hypothesize that for both Pt/MXene-O₃ and Pt/MXene-H₂O the shift of the Pt 4f signal stems from the interaction of Pt with this electron-deficient titania layer, withdrawing charge from interacting Pt particles. Apparently, the interaction of this layered titania with the MXene below makes it different than bulk titania.

At high temperatures (>500 °C) it is known that Ti₃C₂T_x MXene can form Pt-Ti intermetallic phases, which modifies the catalytic activity [14]. We did not observe intermetallic phases (our treatment temperature was 250 °C); thus, this can be ruled out as the cause of enhanced catalytic activity. The ammonia part in ammonia borane is electron-rich and may

interact strongly with the small Pt particles on the oxidised MXene, enhancing the rate of the reaction.

The mechanism of ammonia borane hydrolysis is still unclear. According to Chen *et al*, ammonia borane hydrolysis is expected to proceed through a Langmuir-Hinshelwood mechanism with O–H bond cleavage by Pt-bound NH_3BH_2^* as rate-determining step (where * indicates a free surface site) [56]. Other authors agree that O–H cleavage must be the rate determining step, however, there is no consensus regarding the reacting borane species [57–64]. Increased NH_4^+ concentrations did not influence our hydrolysis reaction much, suggesting B–N bond dissociation is not a critical step for our catalyst and might even not happen at all. It is widely known that ammonia borane hydrolysis depends on the pH of the solution, increasing reaction rate in presence of both acid and base [59, 61, 65, 66]. When NaOH was added to the reaction mixture, we observed a 30% increase in reaction rate, suggesting that OH^- plays a role in the reaction. Both water and aqueous base dissociate reversibly on Pt surface according to equations 2 and 3 [67]. Electron-deficient Pt therefore increases the surface concentration of OH^* , hence directly impacting the rate-determining step. Electron-deficient Pt also enables dissociation of B–H bonds, improving the reaction rate for the Pt/MXene- H_2O and Pt/MXene- O_3 catalysts.



Based on this information, we suggest a variation on the mechanism proposed by Chen *et al*, focussing on O–H bond cleavage and subsequent reaction with NH_3BH_2^* (figure 8). Ammonia borane adsorbs on the Pt surface and one B–H bond dissociates, forming NH_3BH_2^* and H^* (figure 8a). Water adsorbs to the surface and dissociates into OH^* , H^+ and e^- (figure 8b). This H^+/e^- pair reacts with H^* to form hydrogen (figure 8c). Then, the OH^* intermediate combines with NH_3BH_2^* , forming $\text{NH}_3\text{BH}_2(\text{OH})^*$ (figure 8d) which then desorbs. The remaining B–H bonds react analogously. The electron deficient Pt plays a key role in this process.

In summary, we show for the first time that room temperature ozone treatment is a good method for modifying the surface of MXenes. This method gives a thin surface layer of predominantly rutile titania, which usually requires much harsher conditions to form. Pt nanoparticles deposited on this oxidised MXene are more active in ammonia borane hydrolysis than when supported on pristine MXene, due to electronic interactions between the particles and the modified oxide surface.

4. Conclusions

We show that the surface structure of MXene can be modified by a simple controlled treatment with ozone at room temperature. This yields a mildly oxidised surface, which is less oxidised compared to hydrothermal or H_2O_2 treatments. Importantly, the oxidation with ozone creates a thin surface layer of predominantly rutile titania. Conventional heating methods require a high temperature to produce rutile titania. Depositing platinum on this layer results in highly dispersed nanoparticles with an average size less than 1 nm, yet with a more electron-deficient state than that of Pt on non-treated MXene. This means that the electronic environment of a supported metal nanoparticle can be modified by surface oxidation of the MXene. Overall, this electronic modification enhances the catalytic activity of platinum nanoparticles for ammonia borane hydrolysis, giving a faster and more efficient hydrogen production. Considering the growing number of MXene compositions reported, the scope of study for their further derivatisation and application is very broad.

Acknowledgments

We thank ing. N J Geels for N_2 adsorption measurements. T K S was supported by NWO TOP-PUNT grant 718.015.004. Z S was supported by project LTAUSA19034 from Ministry of Education Youth and Sports (MEYS). E V R F and A S E would like to thank financial support by MINECO (Spain) through the projects MAT2017-86992-R and MAT2016-80285-P.

ORCID iDs

Thierry K Slot  <https://orcid.org/0000-0002-6578-4761>

Gadi Rothenberg  <https://orcid.org/0000-0003-1286-4474>

N Raveendran Shiju  <https://orcid.org/0000-0001-7943-5864>

References

- [1] Naguib M, Kurtoglu M, Presser V, Lu J, Niu J, Heon M, Hultman L, Gogotsi Y and Barsoum M W 2011 *Adv. Mater.* **23** 4248–53
- [2] Naguib M, Mochalin V N, Barsoum M W and Gogotsi Y 2014 *Adv. Mater.* **26** 992–1005
- [3] Ng W H K, Gnanakumar E S, Batyrev E, Greer H F, Zhou W, Sakidja R, Rothenberg G, Barsoum M and Shiju N R 2018 *Angew. Chem., Int. Ed.* **57** 1485–90
- [4] Barsoum M W 2013 *MAX Phases: Properties of Machinable Ternary Carbides and Nitrides* (New York: Wiley)
- [5] Hart J L, Hantanasirisakul K, Lang A C, Anasori B, Pinto D, Pivak Y, van Omme J T, May S J, Gogotsi Y and Taheri M L 2019 *Nat. Commun.* **10** 522
- [6] Halim J, Persson I, Moon E J, Kühne P, Darakchieva V, Persson P O Å, Eklund P, Rosen J and Barsoum M W 2019 *J. Phys.: Condens. Matter.* **31** 31165301165301

- [7] Miranda A, Halim J, Barsoum M W and Lorke A 2016 *Appl. Phys. Lett.* **108** 033102
- [8] Zhou S, Yang X, Pei W, Liu N and Zhao J 2018 *Nanoscale* **10** 10876–83
- [9] Jiang Y, Sun T, Xie X, Jiang W, Li J, Tian B and Su C 2019 *ChemSusChem* **12** 1368–73
- [10] Zhang J, Zhao Y, Guo X, Chen C, Dong C-L, Liu R-S, Han C-P, Li Y, Gogotsi Y and Wang G 2018 *Nat. Catal.* **1** 985–92
- [11] Zhang C (John) et al 2019 *Nat. Commun.* **10** 1795
- [12] Wang Y, Ma C, Ma W, Fan W, Sun Y, Yin H, Shi X, Liu X and Ding Y 2019 *2D Mater.* **6** 045025
- [13] Li X et al 2020 *ACS Nano* **14** 541–51
- [14] Li Z et al 2018 *Nat. Commun.* **9** 1–8
- [15] Li Z et al 2018 *Nat. Catal.* **1** 349–55
- [16] Ahmed B, Anjum D H, Hedhili M N, Gogotsi Y and Alshareef H N 2016 *Nanoscale* **8** 7580–7
- [17] Zou G, Guo J, Peng Q, Zhou A, Zhang Q and Liu B 2015 *J. Mater. Chem. A* **4** 489–99
- [18] Cao M, Wang F, Wang L, Wu W, Lv W and Zhu J 2017 *J. Electrochem. Soc.* **164** A3933
- [19] Tang H, Zhuang S, Bao Z, Lao C and Mei Y 2016 *ChemElectroChem* **3** 871–6
- [20] Leitao E M, Jurca T and Manners I 2013 *Nat. Chem.* **5** 817–29
- [21] Eberle U, Felderhoff M and Schüth F 2009 *Angew. Chem., Int. Ed.* **48** 6608–30
- [22] Verma P, Yuan K, Kuwahara Y, Mori K and Yamashita H 2018 *Appl. Catal. B* **223** 10–15
- [23] Cheng H, Kamegawa T, Mori K and Yamashita H 2014 *Angew. Chem., Int. Ed.* **53** 2910–4
- [24] Akbayrak S and Özkar S 2018 *Int. J. Hydrogen Energy* **43** 18592–606
- [25] Hamilton W C, Baker T R, Staubitz A and Manners I 2009 *Chem. Soc. Rev.* **38** 279–93
- [26] Grochala W and Edwards P P 2004 *Chem. Rev.* **104** 1283–316
- [27] Kumar R, Karkamkar A, Bowden M and Autrey T 2019 *Chem. Soc. Rev.* **48** 5350–80
- [28] Liao J, Lu D, Diao G, Zhang X, Zhao M and Li H 2018 *ACS Sustainable Chem. Eng.* **6** 5843–51
- [29] Lu D, Liao J, Li H, Ji S and Pollet B G 2019 *ACS Sustainable Chem. Eng.* **7** 16474–82
- [30] Liao J, Feng Y, Lin W, Su X, Ji S, Li L, Zhang W, Pollet B G and Li H 2020 *Int. J. Hydrogen Energy* **45** 8168–76
- [31] Liu H, Xu C, Lu R, Wang Q, Wu J, Wang Y, Zhang Y, Sun T and Fan G 2019 *Int. J. Hydrogen Energy* **44** 16548–56
- [32] Akbayrak S, Tonbul Y and Özkar S 2020 *ACS Sustainable Chem. Eng.* **8** 4216–24
- [33] Wang H, Xu C, Chen Q, Ming M, Wang Y, Sun T, Zhang Y, Gao D, Bi J and Fan G 2019 *ACS Sustainable Chem. Eng.* **7** 1178–84
- [34] Aijaz A, Karkamkar A, Choi Y J, Tsumori N, Rönnebro E, Autrey T, Shioyama H and Xu Q 2012 *J. Am. Chem. Soc.* **134** 13926–9
- [35] Slot T K, Shiju N R and Rothenberg G 2019 *Angew. Chem., Int. Ed.* **58** 17273–6
- [36] Ramos-Fernandez G, Muñoz M, García-Quesada J C, Rodríguez-Pastor I and Martín-Gullón I 2018 *Polym. Compos.* **39** E2116–24
- [37] Fan G, Li X, Ma Y, Zhang Y, Wu J, Xu B, Sun T, Gao D and Bi J 2017 *New J. Chem.* **41** 2793–9
- [38] Ren X, Lv H, Yang S, Wang Y, Li J, Wei R, Xu D and Liu B 2019 *J. Phys. Chem. Lett.* **10** 7374–82
- [39] Wang S, Zhang D, Ma Y, Zhang H, Gao J, Nie Y and Sun X 2014 *ACS Appl. Mater. Interfaces* **6** 12429–35
- [40] Li Z, He T, Matsumura D, Miao S, Wu A, Liu L, Wu G and Chen P 2017 *ACS Catal.* **7** 6762–9
- [41] Chen W, Duan X, Qian G, Chen D and Zhou X 2015 *ChemSusChem* **8** 2927–31
- [42] Zhou Q, Qi L, Yang H and Xu C 2018 *J. Colloid Interface Sci.* **513** 258–65
- [43] Xu D, Cui Z, Yang J, Yuan M, Cui X, Zhang X and Dong Z 2017 *Int. J. Hydrogen Energy* **42** 27034–42
- [44] Fu -L-L, Zhang D-F, Yang Z, Chen T-W and Zhai J 2020 *ACS Sustainable Chem. Eng.* **8** 3734–42
- [45] Zhao B, Feng K, Wang Y, Lv X, Zheng H, Ma Y, Yan W, Sun X and Zhong J 2017 *Catal. Sci. Technol.* **7** 5135–42
- [46] Zhang J, Chen W, Ge H, Chen C, Yan W, Gao Z, Gan J, Zhang B, Duan X and Qin Y 2018 *Appl. Catal. B* **235** 256–63
- [47] Hsieh B-J, Tsai M-C, Pan C-J, Su W-N, Rick J, Chou H-L, Lee J-F and Hwang B-J 2017 *Electrochim. Acta* **224** 452–9
- [48] Rico-Francés S, Jardim E O, Wezendonk T A, Kapteijn F, Gascon J, Sepúlveda-Escribano A and Ramos-Fernandez E V 2016 *Appl. Catal. B* **180** 169–78
- [49] Kernazhitsky L, Shymanovska V, Gavrilko T, Naumov V, Fedorenko L, Kshnyakin V and Baran J 2014 *Ukr. J. Phys.* **59** 246–53
- [50] Challagulla S, Tarafder K, Ganesan R and Roy S 2017 *Sci. Rep.* **7** 8783
- [51] Zhu J, Tang Y, Yang C, Wang F and Cao M 2016 *J. Electrochem. Soc.* **163** A785
- [52] Dall’Agnese Y, Rozier P, Taberna P-L, Gogotsi Y and Simon P 2016 *J. Power Sources* **306** 510–5
- [53] Wang B, Zhou A, Liu F, Cao J, Wang L and Hu Q 2018 *J. Adv. Ceram.* **7** 237–45
- [54] Hernandez-Mejia C, Gnanakumar S E, Olivios-Suarez A, Gascon J, Greer F H, Zhou W, Rothenberg G and Shiju N R 2016 *Catal. Sci. Technol.* **6** 577–82
- [55] Chen W, Ji J, Feng X, Duan X, Qian G, Li P, Zhou X, Chen D and Yuan W 2014 *J. Am. Chem. Soc.* **136** 16736–9
- [56] Chen W, Li D, Wang Z, Qian G, Sui Z, Duan X, Zhou X, Yeboah I and Chen D 2017 *AIChE J.* **63** 60–65
- [57] Feng K, Zhong J, Zhao B, Zhang H, Xu L, Sun X and Lee S-T 2016 *Angew. Chem., Int. Ed.* **55** 11950–4
- [58] Wang Q, Fu F, Yang S, Martinez Moro M, Ramirez M D L A, Moya S, Salmon L, Ruiz J and Astruc D 2019 *ACS Catal.* **9** 1110–9
- [59] Fu F et al 2018 *J. Am. Chem. Soc.* **140** 10034–42
- [60] Wu H, Luo Q, Zhang R, Zhang W and Yang J 2018 *Chin. J. Chem. Phys.* **31** 641–8
- [61] Wang L, Li H, Zhang W, Zhao X, Qiu J, Li A, Zheng X, Hu Z, Si R and Zeng J 2017 *Angew. Chem., Int. Ed.* **56** 4712–8
- [62] Banu T, Debnath T, Ash T and Das A K 2015 *J. Chem. Phys.* **143** 194305
- [63] Long -L-L, Liu X-Y, Chen -J-J, Jiang J, Qian C, Huang G-X, Rong Q, Zhang X and Yu H-Q 2018 *ACS Appl. Nano Mater.* **1** 6800–7
- [64] Li Y, Hu M, Wang J and Wang W-H 2019 *J. Organomet. Chem.* **899** 120913
- [65] Yao Q, Yang K, Hong X, Chen X and Lu Z-H 2018 *Catal. Sci. Technol.* **8** 870–7
- [66] D’Ulivo L, Spiniello R, Onor M, Campanella B, Mester Z and D’Ulivo A 2018 *Anal. Chim. Acta* **998** 28–36
- [67] van der Niet M J T C, García-Araez N, Hernández J, Feliu J M and Koper M T M 2013 *Catal. Today* **202** 105–13